



## HUMAN TRANSLATION

FTD-ID(RS)T-1058-90      11 April 1991

MICROFICHE NR:    FTD-91-C-000291

POWDER METALLURGY TECHNOLOGY (Selected  
Articles)

English pages:    38

Source:    P/M Technology, Vol. 7, Nr. 4, 1989,  
pp. 213-219; 253-261

Country of origin:    China

Translated by:    Leo Kanner Associates  
F33657-88-D-2188

Requester:    FTD/TTTAV/Robert M. Dunco

Approved for public release; Distribution unlimited.

THIS TRANSLATION IS A RENDITION OF THE ORIGINAL FOREIGN TEXT WITHOUT ANY ANALYTICAL OR EDITORIAL COMMENT. STATEMENTS OR THEORIES ADVOCATED OR IMPLIED ARE THOSE OF THE SOURCE AND DO NOT NECESSARILY REFLECT THE POSITION OR OPINION OF THE FOREIGN TECHNOLOGY DIVISION.

PREPARED BY:

TRANSLATION DIVISION  
FOREIGN TECHNOLOGY DIVISION  
WPAFB, OHIO.

TABLE OF CONTENTS

Graphics Disclaimer ..... 11

Effect of Preliminary Heat Treatment on Microstructure of P/M René  
Superalloy, by Mao Jian, Yu Kelan, Zhou Ruifa ..... 1

Intermetallic Compounds and Their Powder Metallurgy Materials, by  
Ni Ruicheng, Sun Yuan ..... 15

GRAPHICS DISCLAIMER

All figures, graphics, tables, equations, etc. merged into this translation were extracted from the best quality copy available.

EFFECT OF PRELIMINARY HEAT TREATMENT ON MICROSTRUCTURE  
OF P/M RENÉ SUPERALLOY

Mao Jian, Yu Kelan and Zhou Ruifa, Beijing Institute of  
Aeronautical Materials

Abstract: This paper studies the effect of various pre-HIP [heating, isostatic pressure] heat treatment on the size and distribution of prior particle boundary (PPB) carbide precipitates,  $\gamma'$  volume fraction and grain size of HIP billets of René 95 P/M [powder metallurgy] alloy. The possibility of reducing the PPB carbide segregation by using pre-HIP heat treatment was explored. The results show that pre-HIP heat treatment can reduce the degree of PPB carbide segregation, increase the  $\gamma'$  volume fraction, but leave grain size unchanged. This is due mainly to the improvement of pre-HIP powder surface state and the precipitating environment of carbides on PPB.

I. Foreword

Owing to the small and uniform texture of the powder high-temperature alloy without the macroscopic segregations, with few harmful phases and with outstanding properties, powder high-temperature alloys have exhibited their outstanding advantages in the development of novel engine turbine disks and gas compressor disks, among other products. Urgent problems serve to further

exploit the material potential, remove the alloy defects, and to raise the stability of alloy properties.

Accretion of PPB [prior particle boundary] carbides is one of the main defects of powder high-temperature alloys. This is the boundary accretion substance and carbon oxide  $(\text{Ti, Nb})\text{C}_{1-x}\text{O}_x$  formed at PPB with the internally migrating Ti and C during the heating and isostatic pressure (HIP) of oxides with powder surface-enriched with Ti, Cr, Al and surface-adsorbed gaseous oxygen and carbon. These substances hinder the diffusion and bonding of metal particles during HIP, thus forming weak boundary surfaces. Moreover, these weak boundary surfaces, once formed, are very difficult to eliminate in the subsequent heat treatment process; thus, they become the principal initiation sites and passages for the initiation and spread of cracks, and in lowering the plasticity of alloys. Therefore, research to improve the precipitation method of PPB has attracted attention of investigators in China and abroad. At present, there are the following approaches [5-9] to a solution:

1. Use the content of carbon and oxygen in order to reduce the formation of carbide and oxides;

2. At more stable carbide formation elements, such as Nb, Ta, and Hf, among others, carbides are to be formed that are more stable than  $\text{TiC}$ , in particles;

3. Chemical treatment at powder surfaces; gases containing chlorine are used to treat the powders in order to have a depletion effect on the surface of Ti;

4. Vacuum thermodynamic degasification [10]; desorption of oxygen, carbon, and carbon monoxide on the surface of powder particles in order to reduce the nucleation forming factors of PPB precipitation;

5. Powder preheating treatment; powders are subjected first to  $M_{23}C_6$  (or MC) phase stable temperature pretreatment so that uniform, stable, and harmless carbides are formed within the particles. Afterwards, the MC-phase is compacted with stable temperature HIP in order to reduce the optimal formation of nucleating centers of carbides at PPB during HIP; and

6. Thermomechanical treatment; by utilizing the thermoelasticity deformation technique with the low-temperature thermal formation method, thermomechanical treatment methods of extrusion or forging are used to break down the PPB thin films and to improve binding among particles.

This paper discusses mainly the feasibility of powder pretreatment for the reduction of PPB carbide accretion of HIP alloys, as well as the effect on alloy  $\gamma'$  content and crystalline grain sizes. In another article [11], the effect of treatment on the surface state of powder is described, so this description is omitted from this paper.

## II. Experimental Methods

The powder used in the experimentation is the René 95 high-temperature alloy powder prepared by the Crucible Corporation in the United States. The chemical composition of the powder is shown in Table 1.

TABLE 1. Chemical Composition (percent by weight) of René 95 High-Temperature Powder

元素 1	Ni	Cr	Co	Al	Ti	Nb	W	Mo	Fe	Zr	C	O	S	N
分析结果 <sup>2</sup>	余 <sup>4</sup>	12.04	7.68	3.57	2.74	3.63	3.65	3.60	0.21	0.07	0.066	0.010	0.001	0.0047
技术规范 <sup>3</sup>	余 <sup>4</sup>	12~14	7~9	3.3~ 3.7	2.3~ 2.7	3.3~ 3.7	3.3~ 3.7	3.3~ 3.7	<0.5	0.03~ 0.07	0.04~ 0.09	<0.015	<0.015	<0.006

KEY: 1 - Element 2 - Analytical results 3 - Technical norm 4 - Remainders

After dynamic degasification (vacuum  $10^{-8}$  to  $10^{-9}$  x 101kPa) at room temperature, the powder was packed into a stainless steel shell which was welded shut. After 4h of pre-heat treatment at 950, 1000, 1050, 1100 and 1150°C, water quenching was conducted. Finally, HIP formation was obtained after 3h at 1120°C and 97MPa.

When analyzed in terms of the quantitative chemical and metal phases, as well as analysis with transmission electron microscopy, the extent of carbide accretion can be attained in a statistical form. Then the contents of the composition phase can be determined before making a structural analysis.

### III. Experimental Results and Discussion

#### 1. Effect of pretreatment on the PPB status

After direct HIP and pretreatment with different temperatures prior to HIP, Figs. 1 and 2 show the metallurgical textures of the specimens and the corresponding carbide distribution. Upon comparison with alloys of direct HIP, the post-pretreatment HIP alloy had appreciably less accretion of PPB carbides; as the pretreatment temperature was increased, the carbide particles grew in size.

Table 2 shows the statistical results of the effect of carbide quantity on PPB and PPB quantity. In the table, K indicates the PPB quantity of carbide accretion obtained with the unit measurement line. N is the total number of PPB carbides in a unit measurement area. As shown in Table 2, by comparison with the direct HIP alloy, pretreatment not only reduces the amount of PPB contaminated in a unit length, the accretion degree of carbides on PPB is also improved. Comprehensively consider the trend in the effect of the pretreatment temperature, especially

to HIP + H.T alloy, the effect of pretreatment at 1050 to 1100°C is better.

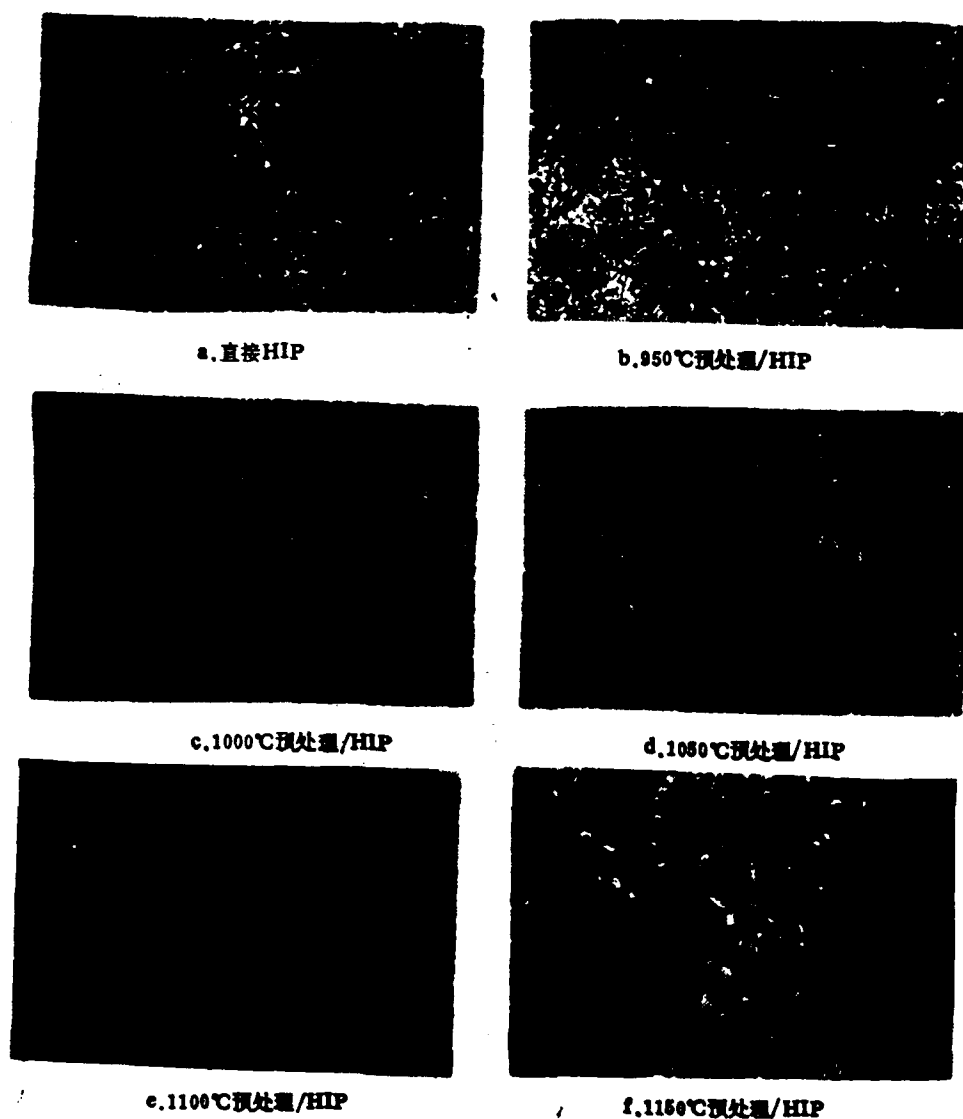


Fig. 1. Metallurgical texture of HIP alloy in different states x1000  
Remarks: a - Direct HIP b - 950°C pretreatment/HIP c - 1000°C pretreatment/HIP d - 1050°C pretreatment/HIP e - 1100°C pretreatment/HIP f - 1150°C pretreatment/HIP

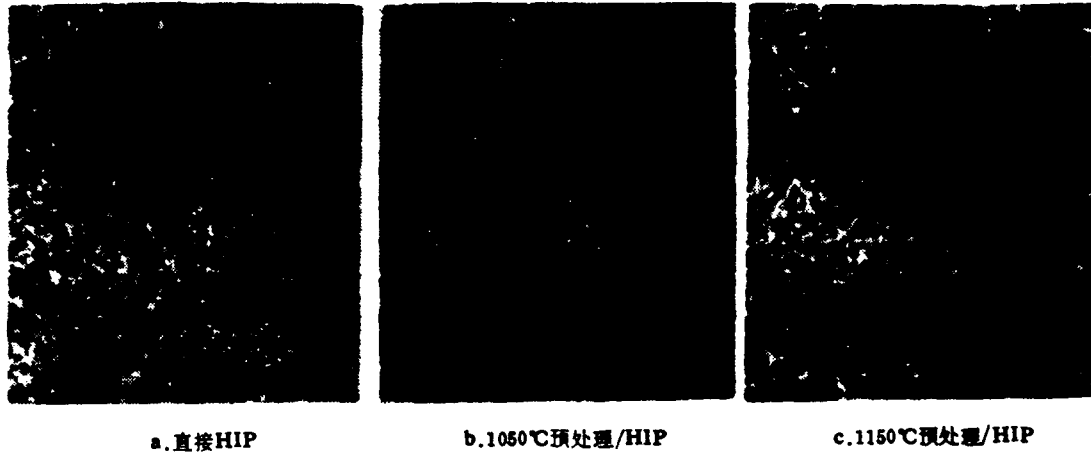


Fig. 2. Distribution of HIP alloy carbides in different states x1000  
 Remarks: a - Direct HIP b - 1050°C pretreatment/HIP  
 c - 1150°C pretreatment/HIP

TABLE 2. Quantitative Measurements of PPB Carbides

参数	2 预处理温度(°C)		3				
	HIP	直接HIP	950	1000	1050	1100	1150
K/mm	HIP	2.02	1.51	1.76	2.01**	1.45	1.65
	HIP+H.T*	2.30	1.85	1.99	1.81	1.87	1.54
N×10 <sup>4</sup> /mm <sup>3</sup>	HIP	82.3	53.7	26.8	90.4**	55.7	59.6
	HIP+H.T	114.0	82.4	83.6	25.9	48.8	38.7

Remarks: \* H.T. -- HIP heat treatment technique: 1120°C/1h oil coating + 870°C/1h air cooling + 650°C/24h air cooling  
 \*\* Possibly caused by experimental errors  
 KEY: 1 - Parameters 2 - Pretreatment temperature (°C)  
 3 - Direct HIP

Fig. 3 shows the distribution state of the boundary carbides observed with a transmission electron microscope. It is apparent that the accretion state of the post-pretreatment boundary

carbides is apparently improved, with broken reticular distribution. It was also discovered during observation that the I-th MC is increased in size with higher pretreatment temperature and increased quantity of MC. As indicated by the analysis of the TEM diffraction dendritic analysis, the boundary carbides are mainly the MC phase, and also the  $M_{23}C_6$  phase. Within the particles, titanium carbonyl was discovered with  $M_6C$  phase with its lattice constant between that of titanium oxide and titanium carbide. As indicated by observation of dislocation configuration (Fig. 4), with rising pretreatment temperatures, the intracrystalline dislocation quantities are increased, forming dislocation cells with subcrystalline boundaries composed of dislocation walls, as well as enlarging accretion of subcrystals. The increase of dislocation numbers is possibly caused by quenching.

## 2. Effect of Pretreatment on Contents and Composition of HIP Alloy $\gamma'$ Phase and Carbides

Table 3 and Figs. 5 and 6 show the analytical results of the chemical phase on the effect of the pretreatment on the content and composition of  $\gamma'$  phase and carbide contents. By comparison with the direct carbide alloy phase, the content of the composition elements (Al, Ti, Ni, Nb) of post-treatment alloy  $\gamma'$  phase is increased, leading to increase of total quantity of  $\gamma'$ ; at the same time, the total quantity of carbides is slightly decreased, mainly with a reduction in  $M_{23}C_6$  content. The variation of pretreatment temperature does not have a marked effect on the precipitate phase content. From the phase composition, whether or not the pretreatment has a little effect on the composition of the MC phase, basically, as  $Ti_{0.35}Nb_{0.55}W_{0.03}Mo_{0.07}C$ , however, the composition of  $M_{23}C_6$  is converted by  $(Cr_{6.4}Ni_{2.3}Co_{14.3})C_6$  of the direct HIP into the  $(Cr_{19.3} to 1.6Ni_{3.9} to 8.4)C_6$  of the post-pretreatment/HIP, and composition varies widely with variation of the pretreatment

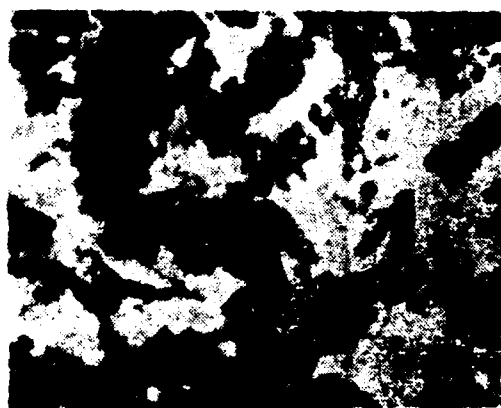
temperature. Further studies are necessary for the cause of the reduction of the  $M_{23}C_6$  content and the variation in composition. No other types of carbides are included, such as  $M_6C$  in the total carbide quantity.



a. 直接HIP ×1000



b. 950°C 预处理/HIP ×3500



c. 1050°C 预处理/HIP ×3500



d. 1100°C 预处理/HIP ×2500

Fig. 3. Boundary carbide states of HIP alloys in different states TEM

Remarks: a - Direct HIP ×1000 b - 950°C pretreatment/HIP ×3500 c - 1050°C pretreatment/HIP ×3500 d - 1100°C pretreatment/HIP ×2500

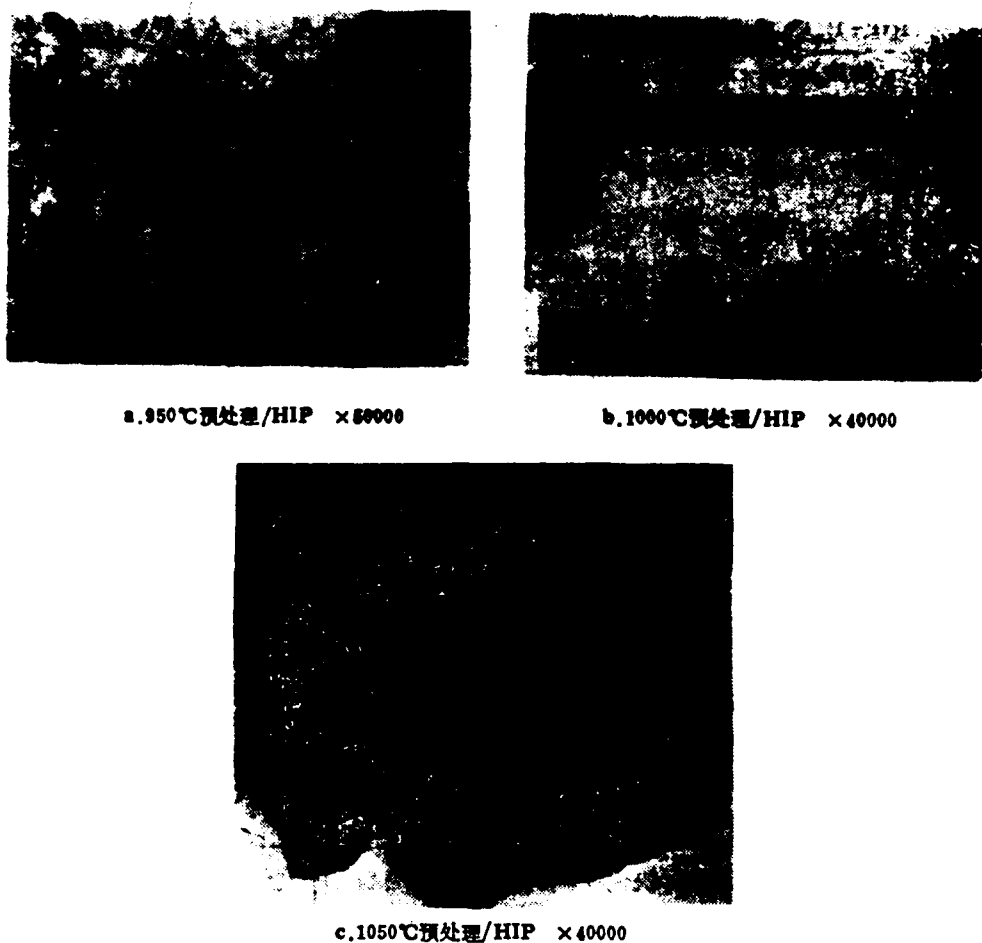


Fig. 4. Dislocation configuration state of different-state HIP alloys TEM  
 Remarks: a - 950°C pretreatment/HIP x50,000  
 b - 1000°C pretreatment/HIP x40,000 c - 1050°C pretreatment/HIP x40,000

### 3. Effect of Pretreatment on the Alloy Crystalline Grain Size

Table 4 shows the results of the effect of pretreatment on the alloy crystalline grain size. It is apparent that pretreatment has only a slight effect on alloy crystalline grain

size; this is because the crystalline grain dimensions are controlled by HIP temperature.

TABLE 3. Variation of  $\gamma'$  and Carbide Content with Pretreatment Temperature (percent by weight)

2 含量 3 析出相	温度(°C)	6 直接HIP	950	1000	1050	1100	1150
$\gamma'$		42.92	45.50	46.09	46.47	46.39	46.12
$\gamma'$ 中含Ni量 <sup>4</sup>		30.66	33.33	33.55	33.91	33.57	33.78
碳化物总量 <sup>5</sup>		0.687	0.556	0.564	0.551	0.551	0.535
MC		0.550	0.529	0.535	0.523	0.520	0.505
M <sub>23</sub> C <sub>6</sub>		0.137	0.027	0.029	0.028	0.031	0.030

KEY: 1 - Temperature (°C) 2 - Content 3 - Precipitate phase 4 - Ni content in  $\gamma'$  5 - Total amount of carbides 6 - Direct HIP

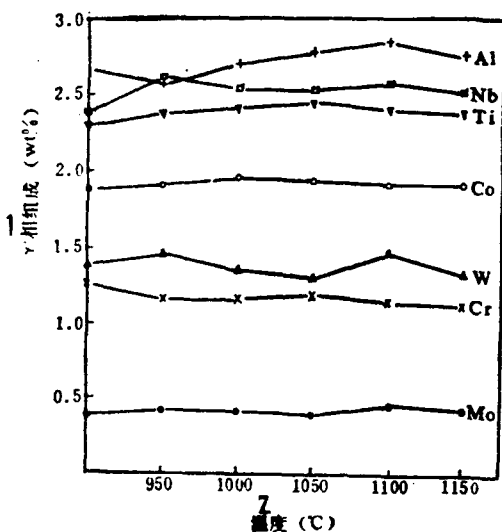


Fig. 5. Variation of  $\gamma'$  phase composition with treatment temperature

KEY: 1 -  $\gamma'$  phase composition (percent by weight) 2 - Temperature (°C)

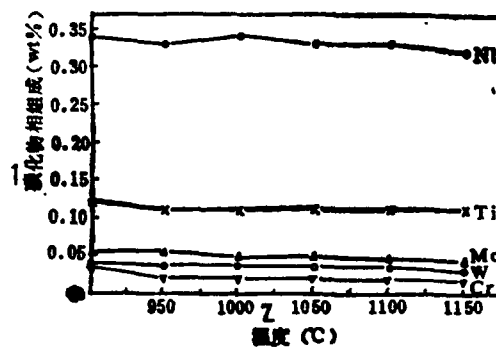


Fig. 6. Variation of carbide phase composition with treatment temperature

KEY: 1 - Composition of carbide phase (percent by weight) 2 - Temperature (°C)

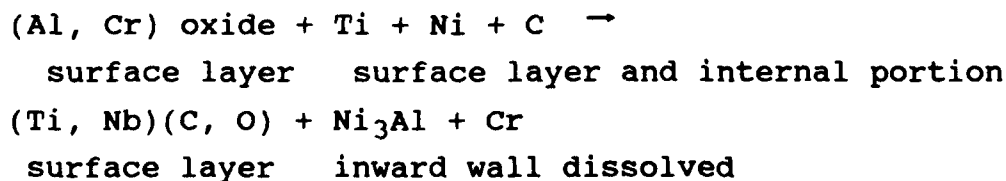
TABLE 4. Effect of Pretreatment on HIP Alloy Crystalline Grain Size

2 晶粒度	1 温度(°C)	直接HIP <sup>5</sup>	950	1000	1050	1100	1150
平均晶粒尺寸(μm) <sup>3</sup>		13.3±1.2	14.0±1.0	14.0±1.0	12.4±1.1	15.0±1.5	14.0±1.0
ASTM级 <sup>4</sup>		9~10	9~10	9~10	9~10	9~10	9~10

KEY: 1 - Temperature (°C) 2 - Crystal grain size  
 3 - Average crystal particle dimensions (μm)  
 4 - ASTM grade 5 - Direct HIP

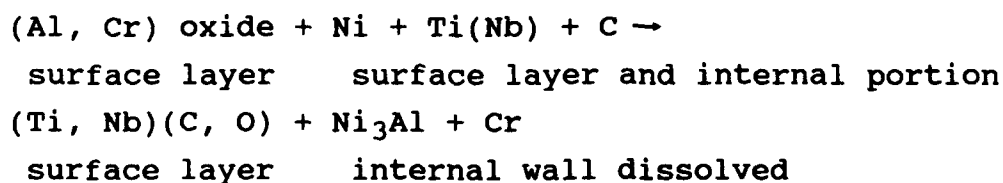
### 3. Discussion

As is well known, the source of effective drive force on alloy compactness by HIP can be viewed in two aspects: one is the surface tension at the clinkering neck of the particle; the second is the externally applied force. The surplus void concentration of the surface tension at the clinkering neck provides the dynamic conditions for atomic diffusion. In addition, creep deformation occurs at the contact zone among particles under the action of external force during HIP, forming a high-energy zone, which provides energy conditions for carbide-shaped nuclei. The boundary surface of low-energy of oxide-oxide existing previously at the particle boundary surface provides the structural conditions for the carbide-shaped nuclei. The dual thermodynamic and dynamic factors allow the carbides at HIP easily form particle contact boundary surface-shaped nuclei to grow [8, 9]. The carbide-shaped nuclei proceed according to the following formulas [1]:



As the clinkering neck grows, in the HIP process the newly formed surface II MC and the powder surface residue I-th MC together continuously distribute at PPB. With the increase of isostatic temperature, and increase of pressure, the driving force of the diffusion is increased, the more serious is the PPB contamination. The experimental situation is consistent with R.D. Kissinger's results [12].

Before HIP, pretreatment was conducted on the powder. At this time, the powder is basically in the loosening state; there is only adherence of particles without growth of the clinkering neck [11]; in addition, the powder lacks the function of external force, basically; the energy and dynamic conditions of the predominant shape of nuclei of carbide do not entirely exist. Besides, the internal portion of the powder for rapid condensation is equivalent to a supersaturated void body. Upon reheating, the surface-enriched elements have a tendency of inward diffusion [11]. At the same time, the powder surface requires elements of enrichment to a certain extent in order to reduce the surface energy. When the surface free energy is at equilibrium with the internal void free energy, elements do not continuously diffuse inward; the surface and internal portion form a uniform and stable carbide. The reaction formula for the formation of the surface carbide is as follows:



The C, O, Ti, and Nb (among other elements) as residue at the surface form the II-th carbide as the upper limit of PPB contamination. In addition, the inward diffusion and reaction of the element increase the  $\gamma'$  content. Before HIP of the powder, the surface and internal portion of the particles form the uniform and stable carbide particles, thus eliminating the

predominantly-shaped nuclei and growth of carbide at the particle boundary surface. This is the internal reason for the reduction of accretion of PPB carbides through pretreatment. Refer to [11] for the effect of powder surface constituents and phase distribution by pretreatment.

#### IV. Conclusions

1. The powder pretreatment technique can appreciably improve the precipitation of PPB carbides and reduce the accretion at the boundaries of HIP René 95 alloy.

2. Powder pretreatment can increase the  $\gamma'$  content of the alloy, reduce the content of carbide  $M_{23}C_6$ , but not change the crystallite grain size.

3. The comprehensive effect is better for pretreatment within the temperature range between 1050 and 1100°C.

#### REFERENCES

- [1] Ingesten, N.G., R. Warren, and I. Winberg, High Temperature Alloy for Gas Turbines, Liege, Belgium, 1982, p. 1013.
- [2] Aubin, C. and J.H. Davison, Superalloys, p. 346, 1980.
- [3] Thamburaj, R. and W. Wallace, Powder Metall. 27/8, 169 (1984).
- [4] Davison, J. A. and G. Aubin, High Temperature Alloy for Gas Turbine, Liege, Belgium, p. 855, 1982.
- [5] Gessinger, G. H., "Powder Metall. of Superalloy-Recent Developments," Proc. 1-st Int. Conf. on P/M Superalloys, Zurich, 1985, No. 8, p. 29.
- [6] Allen, R.E., J.L. Bartos, and D. Aldred, U.S. Patent No. 3890816, 1975.
- [7] Turner, F., Guowai Jinshu Cailiao [Metallic Materials Abroad], No. 8, 29 (1985).

- [8] Dahlen, M., N.-G. Ingesten, and H. Fishmeister, Mod. Dev. in Powder Metall., MPIF/PMI, 1980, Vol. 14, p. 3.
- [9] Dahlen, M. and H. Fishmeister, Superalloys, 449 (1980).
- [10] Wang Wuxiang and Hu He, "Vacuum thermodynamic degasification of powder and improvement of PPB precipitation," Collected Papers of 1987 All-China High-Temperature Alloy Conference (to be published).
- [11] Mao Jian, Yu Kelan and Zhou Ruifa, "Effect of powder pretreatment on the powder surface constituent distribution and phase state," Collected Papers at the 1988 Metal Powder Symposium (to be published).
- [12] R.D. Kissinger et al, Rapidly Solidified Metastable Materials, p. 157, 1984.

## INTERMETALLIC COMPOUNDS AND THEIR POWDER METALLURGY MATERIALS

Ni Ruicheng and Sun Yuan, Shanghai Research Institute of  
Materials

**Abstract:** This paper reviews the fundamental properties, existing problems and possible ways of solving the problems of intermetallic compounds; the paper stresses recent research results and applications of P/M [powder metallurgy] intermetallic compound materials.

A number of outstanding mechanical and physicochemical properties are exhibited by intermetallic compounds, which are an important field attracting research attention in the study of new materials. However, many intermetallic compound materials exhibit serious brittleness at room temperature, thus affecting their applications. The use of powder metallurgical technology in carrying out form processing of brittle intermetallic compounds is an effective fabrication and processing method, whether to enhance material properties or to utilize solidification forming. The article attempts a comprehensive presentation of some basic properties of intermetallic compounds, and some recent studies on powder metallurgical materials.

### I. Definition of Intermetallic Compounds

In the narrow sense, intermetallic compounds are formed

between a metal and another metal. However, some researchers considered recently that the intermediate phases appearing in the semiconductor compounds formed by elements to the left of the semimetallic elements and the nonmetallic element sulfur in the periodic table are all intermetallic compounds. For example, the Ni-Al series, the  $\text{NiAl}_3$  phase,  $\text{Ni}_2\text{Al}_3$  phase,  $\text{NiAl}$  phase, and  $\text{Ni}_3\text{Al}$  phase are typical intermetallic compounds.

On the other hand, generally other treatments are conducted on hydrogenated compounds, carbides and nitrides; one of the reasons is the formation of spacing type compounds due to the position of lattice spacing in the metallic atoms by H, C, and N when a compound is formed. However, the properties of these compounds do not differ widely from those of intermetallic compounds. For instance, carbides or nitrides of Nb, Ta, and W (among other elements) have the similar electroconductivity as metals. Carbides and nitrides of Nb are similarly superconductors as are  $\text{Nb}_3\text{Sn}$ ,  $\text{Nb}_3\text{Al}$ ,  $\text{Nb}_3\text{Ga}$  and  $\text{Nb}_3\text{Ge}$ ; therefore, in some views, carbides and nitrides are included in the definition of intermetallic compounds. In the broad sense, the intermediate phase appearing in the binary element system or a multiple element system mainly of metallic or semimetallic elements is defined as intermetallic compounds.

## II. Properties of Intermetallic Compounds

### 1. Mechanical properties

Generally, it was thought that intermetallic compounds are hard and brittle; however, not all these compounds are so characterized. In the intermetallic compounds with fcc, bcc, and hcp lattices, some compounds have deformability similar to that of conventional metals and alloys; however, when the bond strength is increased among atoms of intermetallic compounds, the crystal structures become complicated; thus, some compounds may

become hard and brittle, not likely to be subject to deformation. The brittleness of many polycrystalline, noncubic sequential alloys (intermetallic compounds) is considered as lacking an adequate slip system, thus not providing deformative compactibility at the crystalline boundaries in random stressed states. Therefore, researchers' expectation of intermetallic compounds with relatively high deformability is often limited to intermetallic compounds of cubic crystals and simple hexagonal crystals.

At room temperature, generally the strength of aluminum compounds is not very high; however, with rise in temperature most sequential alloys (intermetallic compounds), especially the majority of  $L1_2$  structure, their rheodynamic stress has a rapid, abnormal increase, as shown in Fig. 1 [11]. It is especially effective for increased high temperature strength for  $Ni_3Al$  in its alloy of zirconium and hafnium. At  $850^{\circ}C$ , the density compensation yielding strength of the sequential alloys is higher than that of superalloys used industrially (Fig. 2) [2].

The behavior in which rheodynamic stress increases with temperature is believed to be not determined by a single mechanism because the strength peak is related to the conversion temperature of sequential--nonsequential. Sometimes the behavior is related to the structural conversion from one sequential structure to another sequential structure; and sometimes the behavior does not have an apparent relationship to such conversions. Suzuki and his colleagues, as well as Pope et al advanced a series of possible explanations [3, 4].

## 2. Antioxidation and corrosion resistance

For the development of aluminum compounds and other sequential alloys used as structural compounds, the development

leads to research on antioxidation and corrosion resistance of intermetallic compounds.

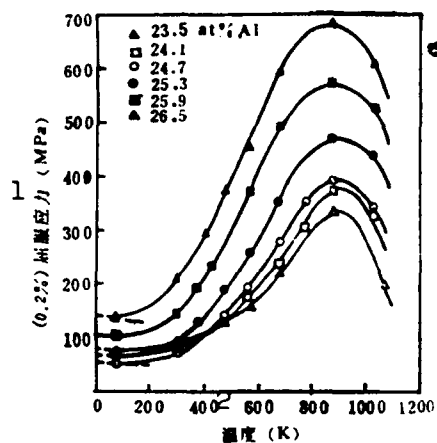


Fig. 1. Effect of constituents to the  $Ni_3Al$  alloy yield strength and temperature  
KEY: 1 - Yield strength  
2 - Temperature

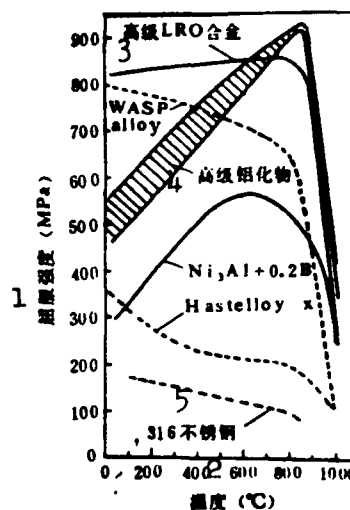


Fig. 2. Comparison of strength between high grade  $Ni_3Al$  and LRO alloys versus traditional alloys  
KEY: 1 - Yield strength  
2 - Temperature

As indicated by some results, aluminum compounds with Ni, Co and Fe as the base have outstanding antioxidation properties. Although relatively brittle, some aluminum compounds, such as  $NiAl$ , can be used for coating layers of gas turbine components; because of good adherence of the  $Al_2O_3$  layer, good antioxidation properties still remain at temperatures in excess of  $1000^{\circ}C$ . For  $Ni_3Al$  with the addition of hafnium, its antioxidation properties at  $1000^{\circ}C$  are better than those of HastelloyX and 316L stainless steel. This advantage is also due to a compact layer of high-adhesion  $Al_2O_3$  film formed at the surface of aluminum compounds. For LRO  $(Fe, Co, Ni)_3V$  alloy, oxidation and stripping of oxide membrane will be caused during an oxidation experiment in air above  $600^{\circ}C$  owing to a lack of Al and Cr in the alloy. However, this kind of alloy can exhibit outstanding anticorrosion in superheated steam of  $540^{\circ}C$ .

In water solution,  $\text{Fe}_3\text{Si}$  exhibits very good corrosion resistance; this is because the compound has a layer with very good adherence, an  $\text{SiO}_2$  protective membrane formed on the surface. With an increase in the Si content in Fe-Si alloys, the dullness begins and electrode potential decreases with widening of the dullness range. For Fe-Si-Al alloys, aluminum can further reduce the dullness potential. As an example,  $\text{Fe}_8\text{Si}$  is incapable of being dulled; however,  $\text{Fe}_8(\text{Al} + \text{Si})$  can be dulled.

From recent work conducted by the authors [5], FeAl alloys have a smaller corrosion proneness compared to that of  $1\text{Cr}_{13}$  stainless steel in 3.5% NaCl solution at room temperature.

### 3. Magnetism [6]

Many intermetallic compounds exhibit outstanding mild and hard magnetic properties. For example,  $\text{Fe}_3(\text{Al}, \text{Si})$  ( $\text{DO}_3$ -type structure, Sendust) as a mild magnetic material contains an alloy (Nimalloy) of  $\text{Ni}_3\text{Mn}$  ( $\text{Li}_2$ -type structure). As for hard magnetic materials, there are MnAl, PtCo, PtFe ( $\text{Ll}_0$ -type structure) and  $\text{SmCo}_5$ , among others. The maximum magnetic permeability of Sendust is  $1.2 \cdot 10^5$ ; with Super-malloy, Sendust is a mild magnetic material with maximum permeability. In the Fe-Al-Si tertiary system, only when the constituents fall within the narrow range of 9 to 10% Si (by weight) and 5 to 6% Al (by weight), do the compound have sharp and high peaks of magnetic permeability. With slight deviations of the constituents, high magnetic permeability cannot be obtained even with  $\text{Fe}_3(\text{Al}, \text{Si})$  phase of the  $\text{DO}_3$ -type structure. The fact that there are outstanding properties that are limited to a very narrow range brings out a hint that later thus-far unknown useful and outstanding properties will be discovered among intermetallic compounds.

### 4. Semiconductor properties

Semiconductors can form semiconductor compounds, such as

ZnS, CdS, GaAs, GaP, PbS, PbTe,  $\text{Bi}_2\text{Fe}_3$ , and  $\text{Sb}_2\text{S}_3$  with elements of Groups IIB and VIB, Groups IIIB and VB, Groups IVB and VIB, and Groups VB and VIB in the periodic table of elements.

Electron transfer between semiconductor energy bands and impurity energy levels can be caused by absorption or emission of light and radioactive rays, in addition to heat energy, thus forming electrons and holes. In the event of recombination, energies can be released in the form of light or in other forms. By utilizing these properties, sensitive elements with a function of converting from electric energy to light energy can be fabricated. By utilizing the p-n junction formed with p- and n-type semiconductors, the functions of current rectification or current amplification can be obtained utilizing the junctions restraining the function of the electron and hole flows, thus fabricating diodes and other transistors.

#### 5. Other Functions and Properties

Like the compound  $\text{Nb}_3\text{Sn}$ , its electric resistance can drop to zero when cooled down to a very low temperature; this is the so-called superconductivity. The critical temperatures and the upper critical magnetic fields of intermetallic compounds such as  $\text{Nb}_3\text{Ge}$ ,  $\text{Nb}_3\text{Ga}$ ,  $\text{Nb}_3\text{Sn}$ , and  $\text{V}_3\text{Ga}$  are relatively high; these are outstanding superconducting materials. Since these intermetallic compounds are hard and brittle, the conventional wire-drawing technique cannot be used. At present, a highly refined method (in situ method) leads to successful fabrication of wires made of  $\text{Nb}_3\text{Sn}$  and  $\text{V}_3\text{Ga}$ .

Although high-critical-temperature superconducting materials have been reported, still the technique is far from practical at present. The above-mentioned intermetallic superconducting compounds are being used in some industrial and scientific-technical fields.

By utilizing other functions and properties of the intermetallic compounds, these compounds can be fabricated into shape memory alloys, hydrogen-storage materials, dental materials, high-brightness electronic wire materials, and catalysts (among other fields).

### III. Intermetallic Compounds in Powder Metallurgy

In powder metallurgy, the constituent segregation caused by the molten casting method is avoided, thus refining texture, which is helpful in overcoming the difficulties in forming brittle materials. In addition, the dimensions and the shape of the intermediate product are close to that of the final product; therefore, powder metallurgy is considered as a promising fabrication technique for intermetallic compounds applied in industrial fields.

In the following, a simple introduction is given to the fabrication technique (mainly on a laboratory scale) and the properties of the intermetallic compound materials from powder metallurgy.

#### 1. Ni<sub>3</sub>Al and NiAl alloys

Ni<sub>3</sub>Al is an intermetallic compound of type L1<sub>2</sub> structure; this is the most important type among intermetallic compounds used as structural material. Studies were made on an alloy with constituents of 12.65% Al, 0.16% B, and the remainder Ni [8]. The alloy is first melted from highly purified nickel, aluminum, and NiB, thus obtaining 4.54kg ingots. Through argon atomization, the ingot is processed into powder, which is enveloped with -140 mesh before being sealed in vacuum welding. At 1150°C, the envelopes are treated for 2h at a heating-isostatic pressure of 103MPa. Some of the blanks formed are cold-rolled at different degrees; some other blanks are annealed

for 1h at 1000°C. At the heating-isostatic pressure state, the blanks are cold-rolled along with annealing (CW 10% + AN). Fig. 3 shows the elongation yield strength of the specimens from the liquid nitrogen temperature (-196°C) to 1000°C. From room temperature to 600°C, the powder metallurgy Ni<sub>3</sub>Al-B alloys exhibit positive rheodynamic stress-temperature relationship; at the temperature of liquid nitrogen, the alloy exhibits higher yield strength than that at room temperature. However, its rupture strength monotonously decreases with rise in temperature (Fig. 4). As revealed by fracture, the powder metallurgical Ni<sub>3</sub>Al alloy is ductile transgranular in shape; therefore, at that time the traditional weak point of brittleness at room temperature for intermetallic compounds does not constitute a problem for the powder metallurgical Ni<sub>3</sub>Al-B alloy. High ductility at room temperature for Ni<sub>3</sub>Al is achieved through microalloy formation. Generally, the ductility of monocrystalline Ni<sub>3</sub>Al is quite satisfactory; polycrystalline Ni<sub>3</sub>Al exhibits much brittleness because of brittle and weak crystal boundaries. The brittleness of polycrystalline Ni<sub>3</sub>Al is due to two factors: one is intrinsic--due to weak binding at crystal boundaries, they are intrinsically brittle and weak compared to the intracrystalline portion. Therefore, highly purified Ni<sub>3</sub>Al exhibits its brittle fracturing at crystal boundaries (without apparent impurity segregation at crystal boundaries). Another type is nonintrinsic: owing to the segregation of impurities which causes brittle crystal boundaries, in Ni<sub>3</sub>Al sulfur has been determined to be one of the trace elements that are capable of causing intensive segregation of crystal boundaries, possibly responsible for the brittleness of Ni<sub>3</sub>Al crystal boundaries. There are two categories of elements with microalloy formation: adjectives of category I are active elements capable of reacting with harmful elements. Through precipitation reaction, the harmful effects are eliminated. The adjectives of category II are elements that are electron donors. For example, in Ni<sub>3</sub>Al boron atoms share

electrons with nickel atoms at crystal boundaries, thus enhancing the binding strength of crystal boundaries. Therefore, small amounts (less than 1%) of added boron can appreciably increase the ductility of Ni<sub>3</sub>Al.

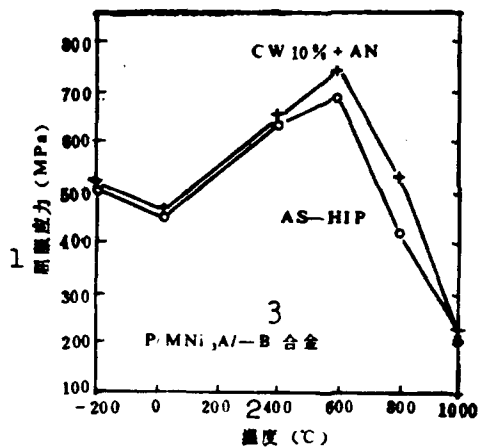


Fig. 3. Relationship between yield strength and temperature of powder metallurgical Ni<sub>3</sub>Al-B alloy  
KEY: 1 - Yield strength (MPa) 2 - temperature (°C)  
3 - P/M Ni<sub>3</sub>Al-B alloy

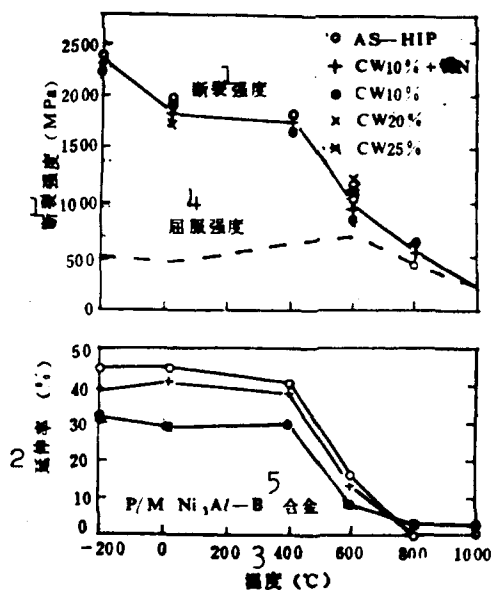


Fig. 4. Relationship between rupture strength and ductility rate, on the one hand, and temperature, on the other, of powder metallurgical Ni<sub>3</sub>Al-B alloy  
KEY: 1 - rupture strength (MPa) 2 - ductility rate (%) 3 - temperature (°C) 4 - yield strength  
5 - P/M Ni<sub>3</sub>Al-B alloy

As pointed out by Chang et al. [9], serious problems may exist when conventional casting and heat treatment are employed to prepare Ni<sub>3</sub>Al-B alloy. First, large ingots are condensed; a slow cooling rate leads to dendritic segregation. Since ductility relies on deviation of stoichiometric constituents and boron content, segregation will cause difficulties in machining following the brittle portion formed in the ingot. In addition, the ductility index of the sequential Ni<sub>3</sub>Al-B alloy monotonously decreases with rise in temperature. The level of ductility in the temperature range of conventional forging is adequate for engineering applications of the materials; however, this ductility level is far from sufficient for heat treatment of the blank forged from ingots. The above-mentioned problems can be overcome by utilizing rapid solidification. Fast cooling eliminates sequential segregation, resulting in uniform stoichiometric composition, thus the material is ductile even in the casting state. The authors used three techniques of rapid solidification for powder preparation: band discarding, atomization and plasma deposition in the fabrication of Ni<sub>3</sub>Al-B alloy. In the atomization technique, 2h of heating-isostatic pressure is carried out at 103MPa and 1150°C after enveloping of -140 mesh powder. In plasma deposition, -400 mesh powder is used. Table 1 shows the properties of the materials thus obtained from these techniques. The following conclusions can be obtained: rapid solidification technique can succeed in fabricating the ductile intermetallic compound Ni<sub>3</sub>Al-B. Powder materials and components made with the heating-isostatic pressure technique have outstanding elongation ductility. The technique also provides an industrially convenient prefabrication method: by using the band discarding method in preparing thin bands, its property can be utilized for selecting by screening the alloy constituents. Plasma deposition can be used to fabricate large and thick parts, as well as wide and thin coating layers. This kind of deposition can exhibit high yield strength and satisfactory elongation ductility. The highest toughening effect

TABLE 1. Room Temperature Elongation Properties of Rapid Solidifying Ni<sub>3</sub>Al-B Alloy

1 合金成分	2 热 处 理	3 2%屈服强度 (MPa)	4 抗拉强度 (MPa)	5 延 伸 率 (%)
	9	6 熔体旋精薄带		
(Ni <sub>75</sub> Al <sub>25</sub> )-1.0B	熔炼后	731	772	0.6
(Ni <sub>75</sub> Al <sub>25</sub> )-1.0B	1100°C/2h	414	420	0.4
(Ni <sub>75</sub> Al <sub>24</sub> )-0.5B	9 熔炼后	627	779	10
(Ni <sub>75</sub> Al <sub>24</sub> )-0.5B	1100°C/2h	262	690	23
	10	7 热等静压粉体		
(Ni <sub>75</sub> Al <sub>25</sub> )-1.0B	热等静压后	496	952	13
(Ni <sub>75</sub> Al <sub>25</sub> )-1.0B	1100°C/2h	503	586	3
(Ni <sub>75</sub> Al <sub>25</sub> )-1.0B	1100°C/2h	496	1062	17
(Ni <sub>75</sub> Al <sub>24</sub> )-0.75B	热静等压后	455	1311	45
	10	469*		
(Ni <sub>75</sub> Al <sub>24</sub> )-0.75B	1000°C/1h	455	1324	46
		8 495*		
	11	等离子淀积		
(Ni <sub>75</sub> Al <sub>24</sub> )-0.75B	沉积后	731	1413	26
		758*		
(Ni <sub>75</sub> Al <sub>24</sub> )-0.75B	1165°C/2h	538	1420	34

\* This value is the upper yield

KEY: 1 - Alloy constituents 2 - Heat treatment  
 3 - 2% yield strength (MPa) 4 - Tensile strength (MPa)  
 5 - Elongation rate (%) 6 - Fine, thin band from rotation of molten body  
 7 - Powder from heating isostatic pressure 8 - Plasma deposition  
 9 - After melting 10 - After heating-isostatic pressure  
 11 - After deposition

on  $\text{Ni}_3\text{Al}$  is at 24% Al (atomic percent) of the constituents. Only when the Al constituent is increased to 25% (atomic percent), annealing brittleness will appear at temperatures higher than  $1100^\circ\text{C}$ .

$\text{NiAl}$  alloy with  $\text{B}_2$  structure is an intermetallic compound, which can be used as a high-temperature structural material. Vedula et al. utilized powder metallurgy in preparing this alloy; they studied the effect of adding the third alloy element [10]. In the preparation of a tertiary alloy, the  $\text{NiAl}$  powder of the previous is blended with powder of the third element additive; the enveloped powder is solidified by hot extrusion or heating-isostatic pressure. For uniform constituents of the alloy, heat treatment is carried out after solidification.

As shown by a heating pressure experiment, at 1300K by adding separately 2% (atomic percent)  $\text{NiAl}$  alloys ( $\text{Ni}_{50}\text{Al}_{48}$ ) of Ti, Ta, and Nb, alloys containing Ta and Nb exhibit greater strengthening than the binary alloys. This type of tertiary alloy elements are only slightly dissolved in the parent phase;

the remainders exhibit in the form of insoluble precipitate enriched with these elements. Therefore, the strengthening mechanism containing Ta and Nb alloy seems to be related to the interaction of dislocation and precipitate. On the TEM micrographs, bowl-shaped bands of dislocations among the submicron particles can be seen; this observation can serve as evidence.

Just as for  $\text{Ni}_3\text{Al}$ ,  $\text{NiAl}$  is brittle at the crystal boundaries as a brittle metallic compound that is not deformed at temperatures lower than  $0.5T_m$  except for compression. However, the refining of crystal grains can allow  $\text{NiAl}$  to exhibit elongation ductility. Schulson et al. studied the relationship between the crystal grain diameter of the  $\text{NiAl}$  polycrystal and its rupture elongation rate [11], as shown in Fig. 5. For the crystal grain diameter below  $20\mu\text{m}$ , the elongation rate rapidly increases; at  $10\mu\text{m}$ , the elongation rate is about 40%. This micro-refining of crystal grains of  $\text{NiAl}$  alloy involves utilizing the recrystallization material obtained by hot extrusion at  $1000^\circ\text{C}$ , and then carrying out hot extrusion at  $500^\circ\text{C}$  (the so-called thermomechanical treatment) to prepare the alloy.

## 2. $\text{Ti}_3\text{Al}$ and $\text{TiAl}$ alloys

$\text{Ti}_3\text{Al}$  is an intermetallic compound of  $\text{DO}_{19}$ -type structure;  $\text{TiAl}$  is an  $\text{Ll}_0$ -type intermetallic compound. Owing to the relatively high aluminum content, a titanium-aluminum compound is lower in density than a titanium alloy, and appreciably lower in density than a nickel-based alloy. Titanium-aluminum compounds have high moduli of elasticity. The modulus of a conventional titanium alloy drops rapidly with temperature; however, for  $\text{TiAl}$  at  $100^\circ\text{C}$  and for  $\text{Ti}_3\text{Al}$  at  $815^\circ\text{C}$ , they exhibit higher moduli than titanium at room temperature. The main shortcoming of titanium-aluminum compounds is their low ductility at room temperature [12]. The authors studied the use of powder metallurgy in the

preparation of Ti<sub>3</sub>Al and TiAl alloys. First, the alloy with the required constituents is cast into rod-shaped small ingots; by utilizing the rotating electrode method, powder is made from the small ingot. The powder is enveloped with Ti-6Al-4V alloy. Hot extrusion (extrusion ratio of 26:1) is conducted on Ti<sub>3</sub>Al at 1230°C and to TiAl at 1400°C; both specimens are prepared with extrusion rods.

Table 2 shows the elongation data at 700°C of Ti<sub>3</sub>Al alloy after different heat treatments. In the extrusion state, the microscopic texture of the alloy is composed of recrystallization texture of antiphase domain with size of approximately 30nm (300Å). At the extrusion state, the alloy strength is the result of the comprehension function of the residual substructures and the antiphase domain caused by extrusion. After heat treatment at 700°C of 126h, the strength is slightly reduced; this is because of the slight restoration of the substructures. With heat treatment at 900°C and 1000°C, complete recrystallization is caused; thus, the strength is lowered more than that in the extrusion state.

TABLE 2. Mechanical Properties of Ti<sub>3</sub>Al Alloy at 700°C

序号 1	热 处 理 2	0.2%屈服应力 <sup>3</sup> (MPa)	极限抗拉强度 <sup>4</sup> (MPa)	5 延 伸 率 (%)	6 截面收缩率 (%)
1	挤压状态 <sup>7</sup>	461	581	3.3	4.8
2	8 挤压+700°C 126h	445	585		
3	9 挤压+900°C 1.75h	348	534	2.5	5.52
4	10 挤压+1000°C 1h	311	508	1.78	3.43

KEY: 1 - Number of sequence 2 - Heat treatment  
 3 - 0.2% yield stress (MPa) 4 - Limiting tensile stress (MPa) 5 - Elongation rate (%) 6 - Contraction rate of cross section (%)  
 7 - Extrusion state 8 - Extrusion + 700°C, 126h 9 - Extrusion + 900°C, 1.75h 10 - Extrusion + 1000°C, 1h

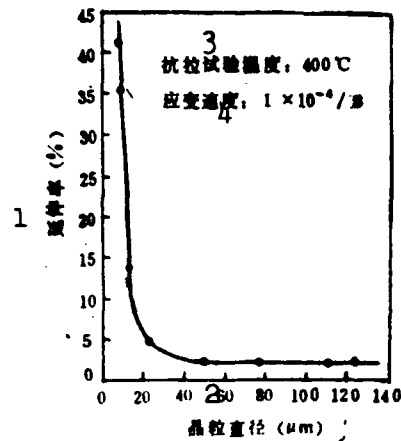


Fig. 5. Relationship between elongation rate and crystal grain diameter of NiAl (51 Ni/49 Al)  
 KEY: 1 - Elongation rate (%) 2 - Crystal grain diameter ( $\mu\text{m}$ ) 3 - Tensile test temperature:  $400^{\circ}\text{C}$  4 - Stress working rate:  $1 \cdot 10^{-4}/\text{s}$

At room temperature the ductility of  $\text{Ti}_3\text{Al}$  alloy is very small; at present, possible methods have been proposed to reduce the slip length and to increase ductility, such as refining the crystal grain, phase transition (such as formation of martensite by quenching), diffusion of the second-phase particles in the parent phase (such as  $\text{Zr}_2\text{O}_3$  in  $\text{Ti}_3\text{Al}$ ) and other methods [13].

Table 3 shows the elongation properties of single-phase TiAl (60% Ti-40% Al) [14]. It can be seen that TiAl exhibits very limited ductility at temperatures below  $600^{\circ}\text{C}$ . As indicated in this study, by using electron microscopy and scanning electron microscopy, fracture at room temperature is cleavage breaking; at  $800^{\circ}\text{C}$ , the apparent cleavage trend of the crystal boundaries is manifested; it is also observed that twinning crystals are also a main deformation shape at this temperature. At  $900^{\circ}\text{C}$ , the ductile fracture form can be seen. As indicated in research, the mobility of  $a/b[112]$  eccentric dislocation controls the plasticity of TiAl; this eccentric dislocation is a composition

of a[011] superdislocations. At temperatures below 630°C, the function under the barrier is basically the same. At temperatures above 700°C, the eccentric dislocations of a/b[112] are not pinned; the activity of a[011] superdislocations increases with rise in temperature. The eccentric dislocations of a/b[125] are also twinning crystal dislocations; above 700°C, twinning becomes an important deformation mode of the TiAl alloy; hence, there is a conversion of ductility brittleness at temperatures between 700 and 800°C.

TABLE 3. Elongation Data of Single-Phase TiAl

温度 1 °C	2 状态	0.2%屈服强度 3 (MPa)	极限抗拉强度 4 (MPa)	断裂应力 5 (MPa)	6 延伸率 (%)	7 截面收缩率 (%)
25	8 挤压	—	—	445.4	~0.1	0.75
600	8 挤压	417.8	—	477.8	0.47	1.65
700	8 挤压	350.2	—	426.8	0.62	1.03
800	8 挤压	301.0	352.3	350.9	10.45	13.8
900	8 挤压	148.2	219.3	216.5	27.6	39.0

KEY: 1 - Temperature, °C 2 - State 3 - 0.2% yield strength (MPa) 4 - Limiting tensile strength (MPa) 5 - Fracture stress (MPa) 6 - Elongation rate (%) 7 - Contraction rate (%) of cross section 8 - Extrusion

As reported recently [15], the room temperature elongation rate of TiAl alloy can be increased by more than 3% by adding Mn.

### 3. FeAl and Fe<sub>3</sub>Al alloys

FeAl alloy has B<sub>2</sub>-type structure while Fe<sub>3</sub>Al alloy has DO<sub>3</sub>-type structure. Since ferro-aluminum alloy has very good antioxidation property, this alloy can be considered for use as high-temperature structural material. The main problem of the alloy is the lack of ductility and poor formation property at room temperature.

The authors applied a sudden-cooling powder preparation technique to fabricate FeAl alloy thin bands in order to study the feasibility [16] to improve ductility at room temperature. Compositions of FeAl sudden-cooling thin band are, respectively, 40, 45, 50, 50.5, and 51% Al (atomic). Fig. 6(a) shows the relationship between the crystal grain size of FeAl alloy, on the one hand, and the heat treatment temperature and compositions, on the other. Fig. 6(b) shows the relationship between the bending test results at room temperature, on the one hand, and the heat treatment and the compositions of the thin band, on the other. In the figure, the range of error falls within the 95% confidence level zone. Heat treatment of FeAl alloy at 775°C leads to a small number of crystal grains to grow; however, with heat treatment at 1000°C, the crystal grains of Fe-40Al and Fe-50Al grow; however, with 45% Al it exhibits resistance to growth of crystal grains. As pointed out by the bending test results of the corresponding FeAl alloy, fracture of the FeAl alloy should decrease with increase in aluminum content. When the aluminum content exceeds the mechanical measurement composition, the fracture strain is maintained constant. For Fe-40Al thin band in the sudden-cooling state, its fracture strength is very high, at 6%. The fracture strain of FeAl alloy with low aluminum composition increases very considerably with heat treatment; however, there is no effect on the FeAl alloy. As indicated by comparing Fig. 6 (a) and (b), there is no direct relationship between crystal grain growth and measured bending ductility. In addition, since thin bands of high bending ductility can be obtained, restraining of crystal boundary breaking, and cleavage breaking within crystals as the main form of breakdown, these factors explain that the above-mentioned heat treatment and deviation from stoichiometry are certainly helpful in strengthening crystal boundaries. With a further understanding of the strengthening mechanism of crystal boundaries in the future, and utilization of the appropriate alloy compounding ratio or heat and mechanical treatment, it can be expected that

FeAl alloy with improved ductility at room temperature will emerge.

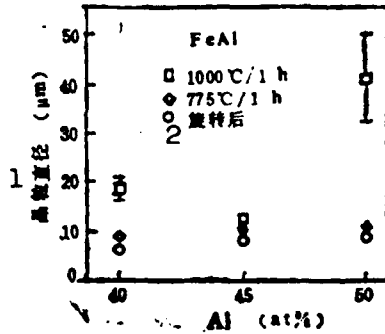


Fig. 6 (a). Relationship between crystal grain size, on the one hand, and the heat treatment temperature and composition of FeAl thin band, on the other  
KEY: 1 - Diameter of crystal  
2 - After rotation

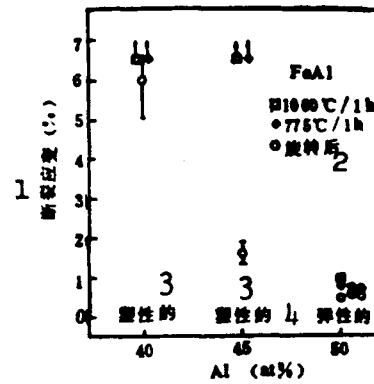


Fig. 6 (b). Relationship between room temperature bending test results of FeAl thin band, on the one hand, and its heat treatment temperature and compositions, on the other  
KEY: 1 - Breaking strain (%)  
2 - After rotation 3 - Plastic  
4 - Elastic

Attention was paid to the Fe-40%Al (atomic) alloy [17] by the NASA Lewis Research Center in the United States because the alloy can be used in gas turbines and the Sterling automotive engine. By adding small amounts of alloying elements of zirconium, molybdenum and boron, the Fe-40Al (atomic) alloy has a creep strength in excess of ordinary stainless steel and is comparable to some iron- and nickel-based superalloy. After alloy formation of the Fe-40%Al alloy, its elongation ductility may be more than 5%.

Developed by the Marko Material Corporation, the ferro-aluminum compound used in turbine engines applies the rapid-solidification technique. The technical constituents of the compound are 13 to 25% Al (by weight) and 3 to 5% TiB<sub>2</sub> (by weight). After processes of band discarding and powder

preparation as well as reheating extrusion solidification, the alloy exhibits its good machining property in the following process of hot forging or hot rolling. This category of low-density alloy has a room-temperature elongation strength of 1380 to 1725MPa; the elongation rate is 3 to 5%; the typical crystal grain size is  $0.5\mu\text{m}$ ; and the average size of  $\text{TiB}_2$  is  $0.1\mu\text{m}$ .

#### 4. Functional materials

With respect to the superconducting intermetallic materials,  $\text{Nb}_3\text{Sn}$  and  $\text{V}_3\text{Ga}$  with the  $\text{Al}_5$ -type structure have found applications; these compounds can be used in various experimental arrangements requiring high magnetic fields. The superconducting crystal temperature  $T_c$  of  $\text{Nb}_3\text{Sn}$  and  $\text{V}_3\text{Ga}$  is, respectively, 18K and approximately 17K. To activate these items of equipment, the  $\text{Nb}_3\text{Sn}$  winding and the  $\text{V}_3\text{Ga}$  winding should be cooled down below  $T_c$ ; therefore, liquid helium (4.2K) is used as the coolant. However, helium is a resource that is short in supply so it is expected that practical high-temperature superconducting materials will be conducted by using liquid nitrogen as the coolant.

In the following, an introduction is made to the application of powder metallurgy to the preparation of  $\text{Nb}_3\text{Sn}$ . First, Nb powder is pressed into blanks for pretreatment with heating; its porosity is approximately 20%. Then the blanks are dipped into molten Sn. Owing to capillary phenomena, the molten Sn penetrates into pores; this clinkering substance is sealed into an envelope for hot extrusion or hydrostatic extrusion to extend the penetrated metal into fibers. With annealing at temperatures between 900 to  $1200^\circ\text{C}$ , diffusion reaction is activated between the Sn fiber and the parent phase of Nb, to form the  $\text{Nb}_3\text{Sn}$  compound. By using this method, the superconducting compound fine filaments of  $\text{Nb}_3(\text{Al}, \text{Ga})$  and  $\text{Nb}_3(\text{Al}, \text{Si})$  can be made.

TiNi shape memory metal is mainly prepared by the melting method. However, by using the self-depression electrode furnace, not all the raw materials are simultaneously converted into an alloy solution, so it is hard to prepare ingots that are uniform in composition without aggregation. If melting is conducted with a graphite crucible high frequency induction furnace, owing to doping of carbon to form carbide, this leads to undesirable effects on the fatigue properties of the alloy. In addition, the cutting and machining properties of TiNi alloy are low; it is quite difficult to fabricate complexly shaped parts. Therefore, efforts were recently made to apply powder metallurgy in fabricating TiNi alloy. The following industrial techniques are in use: alloy powder is used as the starting material and the heating-isostatic pressure technique is used to form and clinker the alloy. Ti powder and Ni powder are used as starting materials for formation and clinkering, or Ti powder and Ni powder are used as starting materials for hot compression together with clinkering. Fabricating single-phase TiNi alloy with density approximating the value achieved in the melting method is difficult with the above-mentioned techniques, unless heating-isostatic pressure is used for forming and clinkering. The reason is as follows: the diffusion rates of Ti and Ni are different, thus generating large numbers of pores. In addition, oxygen in Ti hardly forms a solid solution in the TiNi phase at room temperature, thus becoming  $Ti_4Ni_2O$ , an oxide with undesirable effects on alloy properties. Shangyuan [transliteration of Japanese name] et al. conducted the following research: by utilizing Ti powder and Ni powder as the starting materials and powder metallurgy, TiNi alloy was fabricated [18] with density approaching the value achieved in the melting method. The following raw materials were used in the experiment: Ti powder, -150 mesh, oxygen content 20% (by weight); Ni powder with purity above 99.7%, particle diameter 3 to  $7\mu m$ , and oxygen content 0.15% (by weight). Blend Ti and Ni powders with an atomic ratio of 1:1, and after compressed blanks with clinkering

were formed at 1000°C at 36ks (8.33h), single-phase TiNi alloy can be obtained with a relative density of 85%. If this clinkered substance is subjected to high pressure, hydrostatically, above 203MPa and the pressure is applied for 3.6ks (1h) at 940°C, the relative density can be increased to above 99.8%. By using these techniques, TiNi alloy with the following parameters can be obtained: relative density 100%, oxygen content 0.27% (by weight).

In summation, in research on new materials the study of intermetallic compounds as materials is in its infancy. A great deal of attention has been drawn whether to using these materials structurally or functionally. In particular, intermetallic compounds are promising high-temperature materials with properties between those of high-temperature superalloys and ceramics. Studies on intermetallic compounds in corrosion and grinding resistance are just beginning; these compounds are very promising for use as functional materials, coating layer materials and as composites.

For intermetallic compounds applied as large block materials, the difficulty that needs to be surmounted is brittleness at room temperature. However, this vexing problem can be solved through alloy formation, the addition of second-phase particles, controlling the content of impurity elements, and improving the fabrication and formation techniques. Among these techniques, powder metallurgy for fabricating materials from intermetallic compounds is a very important, if not indispensable, method.

#### IV. Applications of Intermetallic Compounds

Intermetallic compounds have some unique properties that conventional metallic materials do not have. When used as structural materials, these intermetallic compounds exhibit

outstanding properties of high-temperature strength as well as corrosion and grinding resistance. As functional materials, research and development is intensified on compound-semiconductors, compound-superconductors, magnetic alloys, shape memory alloys, hydrogen-storing materials, and alloys for batteries; in addition, intermetallic compounds can also be used as a strengthening phase in composites.

As for the application and prospects of intermetallic compounds, the article has mentioned this subject a number of times. In the following, a simple introduction is given by citing some important examples [9].

1. Jet engine turbine blades fabricated with nickel-based high-temperature alloys.

This type of high-temperature alloy contains as high as 60% (by volume)  $L1_2$ -type (sequential phase face-centered cubic lattice) intermetallic compound  $Ni_3$  (Al, Ti). The high-temperature strength is determined by the specific heat-hardening function of this phase; the heat-hardening function is due to the alternate sliding of {111} plane to the {100} plane, thus thermoactively pinning the spiral dislocations.

2. Engine coating layer with  $B_2$ -type (sequential body-centered cubic lattice) NiAl phase.

When utilizing the NiAl coating layer on turbine blades, oxidation resistance can be improved, thus increasing service life; this usage explains another property of intermetallic compounds, especially certain aluminum compounds and silicon compounds--forming and binding the oxidized surface layer very tightly.

3. Manufacturing of connectors, thermal switches, and blood

coagulation filters by using NiTi-base alloys without welding.

These devices utilize the shape memory property of NiTi and other metallic alloys (such as NiAl, CuZn, and CuZnAl) of the sequential body-centered cubic structure. Through conversion into martensite at low temperatures, the crystal structure becomes more stable. Owing to the reorientation of flake crystals of martensite during cold deformation, restorable strain can be produced. If afterwards the temperature is increased to above the conversion temperature, the structure will be restored to its high-temperature state. Then the deformed part, caused by cold deformation, also returns to its original shape.

#### REFERENCES

- [1] Noguchi, O., Y. Oya and T. Suzuki, Met. Trans. A, 1647 (1981).
- [2] Koch, C. C. et al., High Temperature Ordered Intermetallic Alloys, MRS Symposia Proceedings, Vol. 39, 1984, p. 6.
- [3] Suzuki, T., Y. Oya and D. McVee, Acta Met. 28, 301 (1980).
- [4] Pope, D.P. and S.S. Ez, Int. Met. Rev. 29, 136 (1984).
- [5] Yu Jian, Ni Ruicheng and Sun Yuan, paper to be published, 1988.
- [6] Shankou Zhengzhi and Mayue Youji [Chinese transliterations of Japanese names], Intermetallic Compounds, Industrial News Agency for Japanese journals, 1984.
- [7] Kumao De and Tianjing Yingyong [Chinese transliterations of Japanese names], Metals 54/10, 6 (1984).
- [8] Chang, K.-M., S.C. Huang and A.I. Taub, Report No. 85CRD040, 1985.
- [9] As in [2], p. 336.
- [10] As in [2], p. 411.
- [11] Schulson, E.M. and D.R. Baker, Scr. Metall. 17, 519 (1983).
- [12] Sastry, S.M. and H.A. Lipsitt, Met. Trans. 8A, 299, 1543 (1977).

- [13] As in [2], p. 437.
- [14] Lipsitt, H.A. and D. Shechtman and R.E. Schafrik, Met. Trans. 6A, 1991 (1975).
- [15] Qiaoben Jianji, Tufei Chunfu and Qianben Dezang [Chinese transliterations of Japanese names], Plastic Deformation of Regular Alloys and Intermetallic Compounds, Japan Metals Association, [six Japanese characters that remain to be translated], 1986, p. 17.
- [16] As in [2], p. 429.
- [17] Metal Progress, No. 1, 61 (1986).
- [18] Shangyuan Zhongzhao [Chinese transliteration of Japanese name] et al., Powder Metallurgy of Powders, [three Japanese characters that remain to be translated] 31/1, 146 (1984).
- [19] Schulson, Erland M., The Inter. J. of Powder Metallurgy 23/1, 25.

DISTRIBUTION LIST

DISTRIBUTION DIRECT TO RECIPIENT

<u>ORGANIZATION</u>	<u>MICROFICHE</u>
C509 BALLISTIC RES LAB	1
C510 R&T LABS/AVEADCOM	1
C513 ARRADCOM	1
C535 AVRADCOM/TSARCOM	1
C539 TRASANA	1
Q591 FSTC	4
Q619 MSIC REDSTONE	1
Q008 NTIC	1
E053 HQ USAF/INET	1
E404 AEDC/DOF	1
E408 AFWL	1
E410 AD/IND	1
F429 SD/IND	1
P005 DOE/ISA/DDI	1
P050 CIA/OCR/ADD/SD	2
AFTT/LDE	1
NOIC/OIC-9	1
CCV	1
MIA/PHS	1
LLYL/CODE L-309	1
[REDACTED]	1
NSA/T513/IDL	2
ASD/FTD/TTIA	1
FSL	1